Flow in shock tubes with area change at the diaphragm section*

By R. A. ALPHER and D. R. WHITE
General Electric Research Laboratory, Schenectady, New York

(*Received* 27 *August* 1957)

SUMMARY

This paper describes theoretical and experimental studies of the effects on shock tube flows of a monotonic convergence at the diaphragm section. Systematic flow equations are developed for tubes of uniform bore and tubes having either a monotonic convergence or a convergence–divergence in the diaphragm section. Except across the shock front itself, isentropic processes and ideal-gas behaviour have been assumed. Simplified procedures are presented for predicting the ideal-flow parameters over a wide range of operating conditions, as well as for comparing straight and convergent tubes. Such comparisons made by other investigators are found to be incomplete or in error. The experiments described utilize a very simple device for altering the diaphragm section convergence and a multi-station measurement of shock velocity. The expected effect of convergence is verified over a wide range of Mach numbers. Even at Mach numbers where the processes of shock formation can no longer be ignored, it is found that the relative performance between a uniform and convergent tube is preserved.

INTRODUCTION

The basic shock tube is one of uniform cross-section throughout, in which the rapid removal of a diaphragm separating two gases at different pressures leads to the generation of a shock wave in the region of lower pressure. The regions initially at high and low pressure are designated as driver and driven sections respectively. It has now been well established experimentally that if all other initial conditions are equal, one will realize a stronger shock wave in a tube having in the diaphragm region an area reduction from driver to driven section than in a tube of uniform bore. So-called convergent shock-tube flows have been considered by Bannister & Mucklow (1948), Lukasiewicz (1952), Resler, Lin & Kantrowitz (1952), Wallace & Mitchell (1953), Wallace & Nassif (1954), Hooker & White (1955), and Alpher & White (1957). This last reference contains the theoretical work of this paper together with more extensive derivations and calculations.

* A preliminary account of this work was given at the 1957 Annual Meeting of the American Physical Society in New York City.

In this paper we shall develop a general idealized theory of shock-tube flows, valid for uniform, convergent, or convergent–divergent tubes, whether operated in the subsonic or supersonic cold-flow regimes. Experiments will be described which show the difference between uniform and convergent tubes to be as predicted over a wide range of Mach numbers, even though with increasing shock strength an increasing deviation from absolute predictions of the theory is noted.

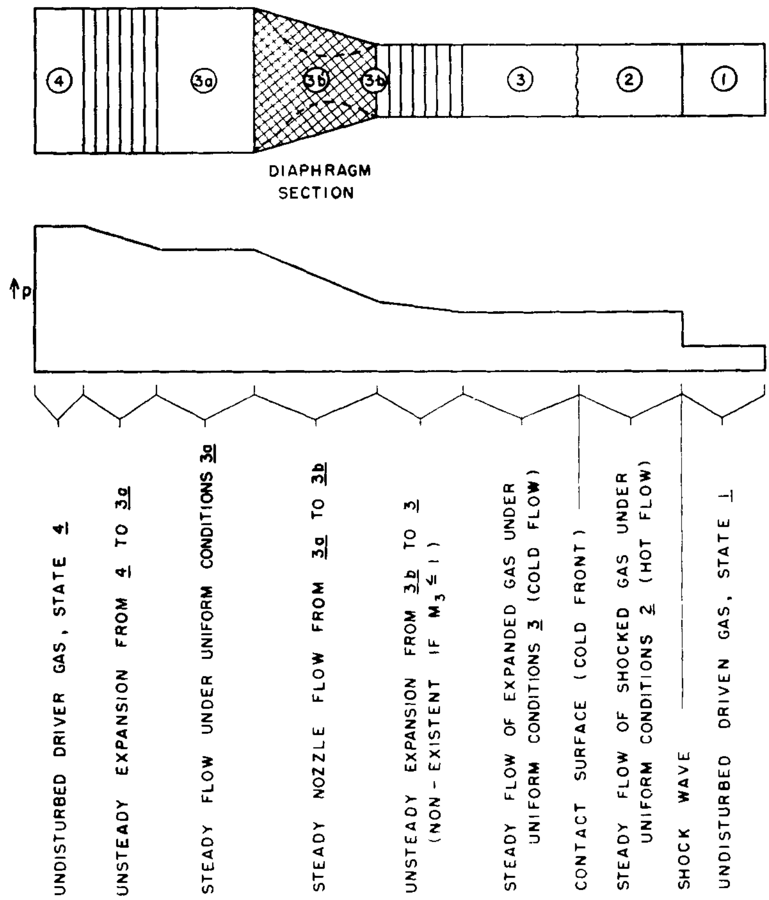

Figure 1. Schematic diagram of shock tube with convergent geometry at the diaphragm section. The dashed lines in the diaphragm section denote a convergent–divergent geometry with minimum area at $3b'$. The pressure distribution is, of course, only symbolic.

The model of the flow situation which has been employed is given in figure 1. After diaphragm removal, energy is extracted from the driver gas through an unsteady expansion from state 4 to state $3a$. The transition section presents three possibilities. If it is uniform, i.e. if it connects equal areas, states $3a$ and $3b$ coalesce and denote the state at the diaphragm location. If the cold flow is supersonic, this state is the point in an unsteady expansion at which the Mach number becomes unity. If the transition is montotonically convergent, the flow from $3a$ to $3b$ is steady nozzle flow, and the convergent flow at $3b$ may be either subsonic or sonic. Following $3b$ one has either uniform flow in state 3 with $M_3 \leqslant 1$ or an unsteady supersonic expansion to state 3 with $M_3 > 1$. Finally, if the transition section is convergent–divergent, i.e. if $3b'$ represents a minimum area, one has either a subsonic or supersonic nozzle between states $3a$ and $3b$. In the supersonic case the exit flow at state $3b$ may be subjected to a further unsteady expansion to state 3. Boundary-layer effects, attenuation and the process of shock formation have not been considered. The driver gas is treated isentropically, and departures from ideality are not explicitly considered for the shocked gas. As will be seen, it is a simple matter to modify this presentation to include the real changes in the driven gas states.

Basic calculations involve determining, for initially given gases and thermodynamic states in the driver and driven sections (i.e. the pressures p_1 and p_4, sound velocities a_1 and a_4, and specific heat ratios γ_1 and γ_4) the resultant shock strength and the thermodynamic state of both the expanded and shocked gases.

Theory

Uniform shock tube

The situation in a uniform tube is sufficiently well known that it need have only brief mention. One wants to relate the initial pressure ratio across the diaphragm, $p_4/p_1 = z$, to the pressure ratio across the shock (i.e. the shock strength $p_2/p_1 = y$) or alternatively to the shock Mach number M_s. In the uniform tube there is a continuous unsteady expansion from state 4 to state 3. If $M_3 \geqslant 1$ one has sonic flow at the diaphragm location. The particle velocity imparted by an unsteady expansion from p_4 to p_3, where we note that $p = k\rho^\gamma$ and that $u_4 = 0$, can be written (see Liepman & Puckett (1947), p. 461)

$$u_3 = \int_{\rho_3}^{\rho_4} \left(\frac{dp}{d\rho}\right)^{1/2} \frac{d\rho}{\rho} = \frac{2a_4}{\gamma_4 - 1}\left[1 - \left(\frac{p_3}{p_4}\right)^{(\gamma_4-1)/2\gamma_4}\right]. \tag{1}$$

This velocity can be subsonic, sonic or supersonic in value. The flow or particle velocity behind the normal shock is determined from the shock Hugoniot; or, if treating the shocked gas as ideal gives an adequate approximation, then the Rankine–Hugoniot relations give

$$\frac{u_2}{a_1} = \frac{2^{1/2}(y-1)}{\{\gamma_1[(\gamma_1-1)+(\gamma_1+1)y]\}^{1/2}} = \frac{2}{\gamma_1+1}\frac{M_s^2-1}{M_s}. \tag{2}$$

We can combine (1) and (2) since at the interface between shocked and expanded gas we must have $u_3 = u_2$ and $p_3 = p_2$. Solving for z yields, for the uniform tube,

$$z = y\left(1 - \frac{a_1}{a_4}\frac{\gamma_4 - 1}{2}\frac{u_2}{a_1}\right)^{-2\gamma_4/(\gamma_4-1)}. \tag{3}$$

Tube with diaphragm section area change

Relationships between z and y or M_s for the tube with an area change in the diaphragm section are obtained as for the uniform tube. Referring again to figure 1, one proceeds as before to connect the shock front with the driving gas by matching pressure and flow velocity at the contact surface, except that now steady or unsteady processes, as the case may be, must be considered at the diaphragm section. Consider the general case of a convergent–divergent diaphragm section. When the shock-tube flow is established, the pressure ratio z may be expanded as follows (see figure 1):

$$z_c = \frac{p_4}{p_1} = \frac{p_4}{p_{3a}}\frac{p_{3a}}{p_{3b'}}\frac{p_{3b'}}{p_{3b}}\frac{p_{3b}}{p_3}\frac{p_3}{p_2}\frac{p_2}{p_1}. \tag{4}$$

Here the suffix c refers to the non-uniform tube, whereas suffix s will be used to refer to the uniform tube. The various pressure ratios in (4) can be interpreted directly. Thus p_4/p_{3a} is that ratio required to accelerate the driver gas by an unsteady expansion from rest to Mach number M_{3a}. The ratio $p_{3a}/p_{3b'}$ is that required to bring the driver gas by a steady expansion from M_{3a} to $M_{3b'}$. One can introduce the area ratio $A_4/A_{3b'}$ into $p_{3a}/p_{3b'}$ by using the condition of conservation of mass. Expansion from $3b'$ to $3b$ also will be a steady process, supersonic or subsonic according as the flow at $3b'$ has become sonic or not. (By our restriction to isentropic channel flow for the driver gas, we exclude that range of z which leads to an over-expansion for a convergent–divergent section.) In either event the ratio $P_{3b'}/P_{3b}$ is that required to bring the gas by a steady expansion from $M_{3b'}$ to M_{3b} through an area ratio $A_{3b'}/A_{3b}$. The ratio p_{3b}/p_3 is then that needed for an unsteady expansion from M_{3b} to M_3. At the contact surface, $p_3 = p_2$, and p_2/p_1 is defined as the shock strength y. Equation (4) can therefore be written as

$$z_c = \left\{\left[1+\frac{\gamma_4-1}{2}M_{3a}\right]\left[\frac{2+(\gamma_4-1)M_{3b}^2}{2+(\gamma_4-1)M_{3a}^2}\right]^{1/2}\left[\frac{2+(\gamma_4-1)M_3}{2+(\gamma_4-1)M_{3b}}\right]\right\}^{2\gamma_4/(\gamma_4-1)} y. \tag{5}$$

Since this relation involves M_3, M_{3a} and M_{3b} as well as z_c and y, we require additional relationships. One of these involves the overall area ratio in the transition section, which can be written as follows, regardless of whether $M_{3b'}$ is subsonic or sonic or whether $3b'$ is a section of minimum area or an undistinguished section in a monotonic convergence:

$$\frac{A_4}{A_1} = \frac{M_{3b}}{M_{3a}}\left[\frac{2+(\gamma_4-1)M_{3a}^2}{2+(\gamma_4-1)M_{3b}^2}\right]^{(\gamma_4+1)/2(\gamma_4-1)}. \tag{6}$$

The second relation we require connects M_s with M_3, M_{3a} and M_{3b}. One expands M_3 in the same way as z_c in (4); thus

$$M_3 = \frac{u_3}{a_3} = \frac{u_2}{a_3} = \frac{u_2}{a_1}\Big/\frac{a_3}{a_1} = \frac{u_2}{a_1}\Big/\left(\frac{a_3}{a_{3b}}\frac{a_{3b}}{a_{3a}}\frac{a_{3a}}{a_4}\frac{a_4}{a_1}\right). \tag{7}$$

Substituting for the sound velocity ratios, we obtain

$$M_3 = \left[\frac{a_1}{u_2}\frac{a_4}{a_1}g^{(\gamma_4-1)/2\gamma_4} - \frac{\gamma_4-1}{2}\right]^{-1}, \tag{8}$$

where the quantity g, which we call an 'equivalence' factor (see next section), was first used by Resler, Lin & Kantrowitz (1952). It is defined as

$$g = \left\{\left[\frac{2+(\gamma_4-1)M_{3a}^2}{2+(\gamma_4-1)M_{3b}^2}\right]^{1/2}\left[\frac{2+(\gamma_4-1)M_{3b}}{2+(\gamma_4-1)M_{3a}}\right]\right\}^{2\gamma_4/(\gamma_4-1)}. \tag{9}$$

Using g, one can rewrite (5) as

$$z_c = \frac{y}{g}\left[1+\frac{\gamma_4-1}{2}M_3\right]^{2\gamma_4/(\gamma_4-1)} = \frac{y}{g}\left[1-\frac{u_2}{a_1}\frac{a_1}{a_4}\frac{\gamma_4+1}{2}g^{-(\gamma_4-1)/2\gamma_4}\right]^{-2\gamma_4/(\gamma_4-1)}. \tag{10}$$

Equations (6) to (10) enable the calculation of shock-tube flows with a convergent or convergent–divergent diaphragm section, in the case of subsonic, sonic or supersonic cold flow. The results for a uniform tube are recovered by noting that with $A_4/A_1 = 1$, one has $M_{3a} = M_{3b}$ with $g = 1$.

For subsonic cold flow (the assumption of isentropy excludes a transition to subsonic flow through a shock), the transition section is a subsonic nozzle with $M_{3b} = M_3$, $p_{3b} = p_3$ and $a_{3b} = a_3$. Equations (6), (8) and (9) reduce to three simultaneous equations in g, M_3 and M_{3a}, which can be solved by iteration with an *ab initio* choice of a_4, a_1 and M_s. In this subsonic case, only the ratio A_4/A_1 enters, and the existence of a minimum section $A_{3b'}$ is irrelevant.

For supersonic cold flow, $M_3 \geqslant 1$, one must have $M_{3b'} = 1$ (or $M_{3b} = 1$ if the section is monotonically convergent so that $A_{3b} = A_1$ is the minimum area). The usual relationships between area ratio and Mach number in supersonic nozzles apply, as used in obtaining (5), to give M_{3a} and M_{3b}. From these M_3, g, and z_c follow.

Computation of shock-tube parameters

The procedure used in developing the shock-tube equations suggests a rather simple graphical means of solving the equations for a given tube. The reader will recall that the shocked gas and the driver gas are connected by matching pressure and velocity across the contact surface. The graphical material can be divided into that pertaining to the driver and that to the driven gases, the one being independent of the other except as matched at the contact surface. The advantages of this are made clear in the following.

The shocked gas may be characterized by a plot of either shock strength y or shock Mach number versus u_2/a_1, where u_2 is the flow velocity imparted by the shock. Such curves may be computed from (2) for ideal gases, but require a knowledge of the shock Hugoniot if the shock strength is sufficient to merit this (see, for example, Döring 1949, Alpher 1957, or Lighthill 1957).

The driver gas is brought into the calculation in the following way. A statement of A_4/A_1, γ_4 and a_4 determines the equivalence factor g as a function of $u_3/a_4 = u_2/a_4$. Plots of g *vs* $(u_2/a_1)(a_1/a_4)$ are given in figure 2 for $\gamma_4 = 5/3$ and in figure 3 for $\gamma_4 = 7/5$ for both subsonic and supersonic cold flow. It may be noted that for $M_3 < 1$ these plots apply either to a monotonically convergent or a convergent–divergent transition section, while for $M_3 > 1$ they hold only for the monotonically convergent section, since in this latter case M_{3b} (see (9)) is taken as unity. Figure 4 is a plot of g *vs* γ_4 for various values of A_4/A_1 in the case $M_3 \geqslant 1$. Again the plot holds for monotonic convergence, since M_{3b} is taken as unity. Such a plot is of use with combustion drivers, in which helium or hydrogen plus the products of hydrogen–oxygen combustion give an intermediate γ_4 value.

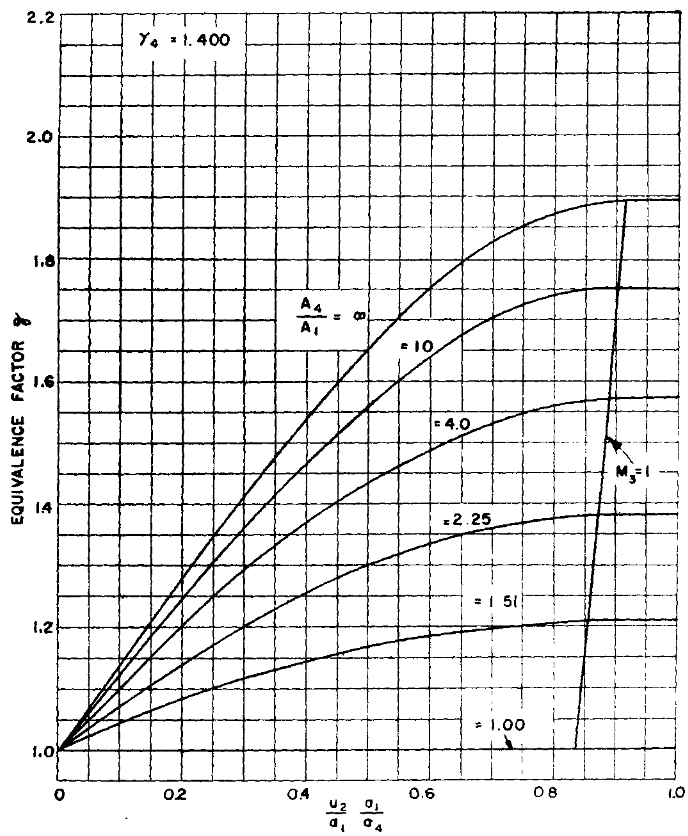

Figure 2. The equivalence factor g *vs* $(u_2/a_1)(a_1/a_4)$ for a selection of area ratios, with $\gamma_4 = 1{\cdot}4$. The connecting line at the right of the curves is the locus of g values for which the cold flow is sonic ($M_3 = 1$). For larger values of $(u_2/a_1)(a_1/a_4)$ corresponding to $M_3 > 1$, g is constant and equal to the values on this sonic line.

The usual calculation to be performed for a shock tube is the determination of the diaphragm pressure ratio z required to produce a shock of given strength y. One is given γ_1, γ_4, a_1, a_4, A_4/A_1 and y. From y the flow velocity u_2/a_1 is computed. The appropriate equivalence factor is then read from figures 2, 3 or 4. Finally from figure 5 (which is a plot of equation (10)) one reads gz/y, whence z is determined. It may be noted that the quantity z/y is the ratio of pressures through which the driver gas expands. When one has at hand a tube with fixed A_4/A_1, then curves of z/y *vs* u_2/a_4 may be prepared which incorporate the appropriate equivalence factor. Such curves are particularly useful when various gases are to be used or when high temperature shock Hugoniots are to be taken into account.

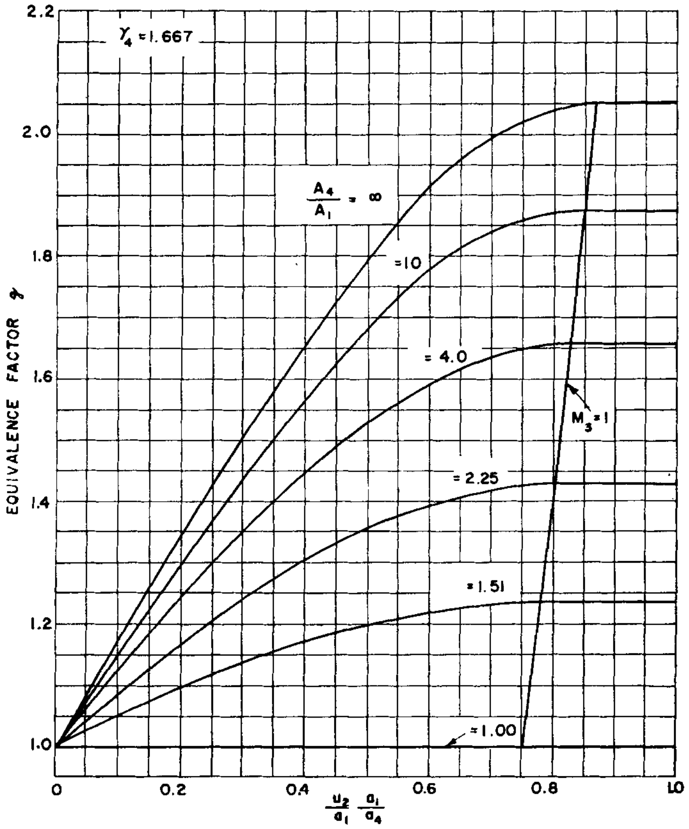

Figure 3. The equivalence factor g *vs* $(u_2/a_1)(a_1/a_4)$ for a selection of area ratios with $\gamma_4 = 1{\cdot}667$. The connecting line at the right of the curves has the same meaning as in figure 2.

To illustrate the results of such calculations, we have prepared figure 6, which gives the diaphragm pressure ratio required to produce given shock Mach numbers for helium driving into ideal argon (electronic excitation and ionization are negligible up to $M \doteqdot 10$ in argon) for several area ratios. An ideal y *vs* M_s curve is included for reference.

'Gain' factors

Although the use of a convergent transition section may have such advantages as smoothing out flow irregularities associated with combustion driving, as well as locating the diaphragm where it will not choke the flow if it does not open completely, the main reason for using such sections is that they provide an easy way of getting a stronger shock, other things being equal. It is therefore pertinent to consider various measures of the 'gain' to be realized with a convergent tube as compared with a uniform tube. One such measure is the ratio $G_M = z_s/z_c$, where z_s and z_c are the respective values for a uniform and a convergent tube in which the same Mach number is achieved, all other things being equal. The simplest way of obtaining G_M, other than computing it from (3) and (10), is to read off z for the given A_4/A_1, and for $A_4/A_1 = 1$ for a given M_s, from a plot such as figure 6; the ratio in then computed between these z values. As may be readily shown from the analytical expression, the factor G_M becomes infinite, as does z_s, when M_s is increased without limit.

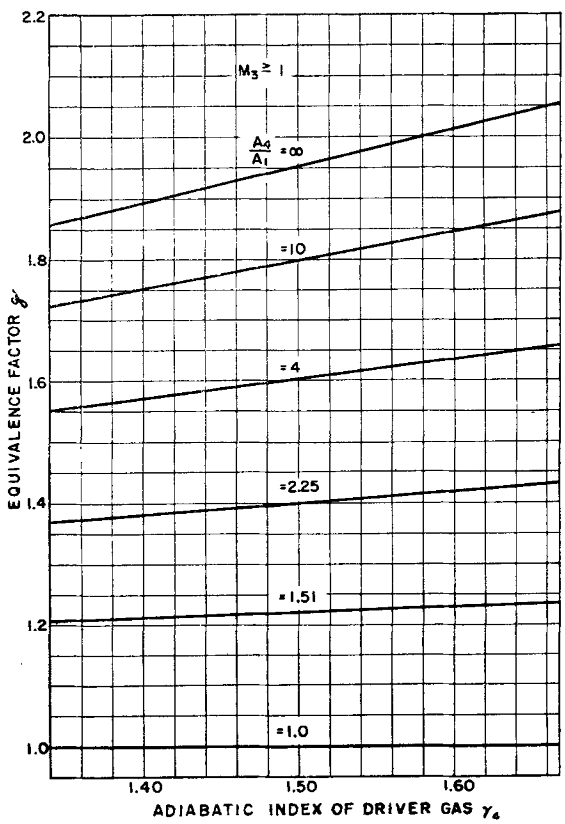

Figure 4. Limiting value of the equivalence factor g, corresponding to sonic or supersonic cold flow, *vs* γ_4 for various convergence area ratios in a monotonically converging tube.

A second measure of gain, G_z, may be defined as the ratio of the shock Mach number achieved in a convergent section tube to that in a uniform tube for the same diaphragm pressure ratio, all other things being equal. Analytic expression of such a factor is not possible, but values of G_z are readily obtained from plots such as figure 6 by reading the values of M_s for the given A_4/A_1 and for $A_4/A_1 = 1$ at a given z. It is not difficult to show that for ideal gas behaviour G_z approaches a limiting value $g^{(\gamma_4-1)/2\gamma_4}$ as z increases without limit. These limiting values are implicit in table 1, which will be explained immediately below. Examination of equations (3), (8), and (10) indicates that the diaphragm pressure ratio and the cold flow Mach number both become infinite at a finite value of u_2. Hence, under ideal conditions (as represented by equation (2)), there is a maximum shock strength attainable in a given tube. Table 1 gives maximum values of the shock Mach number (i.e. the values for $p_4/p_1 \to \infty$) for various values of A_4/A_1, both for the temperature ratio $T_4/T_1 = 1$ and for $T_4/T_1 = 2$.

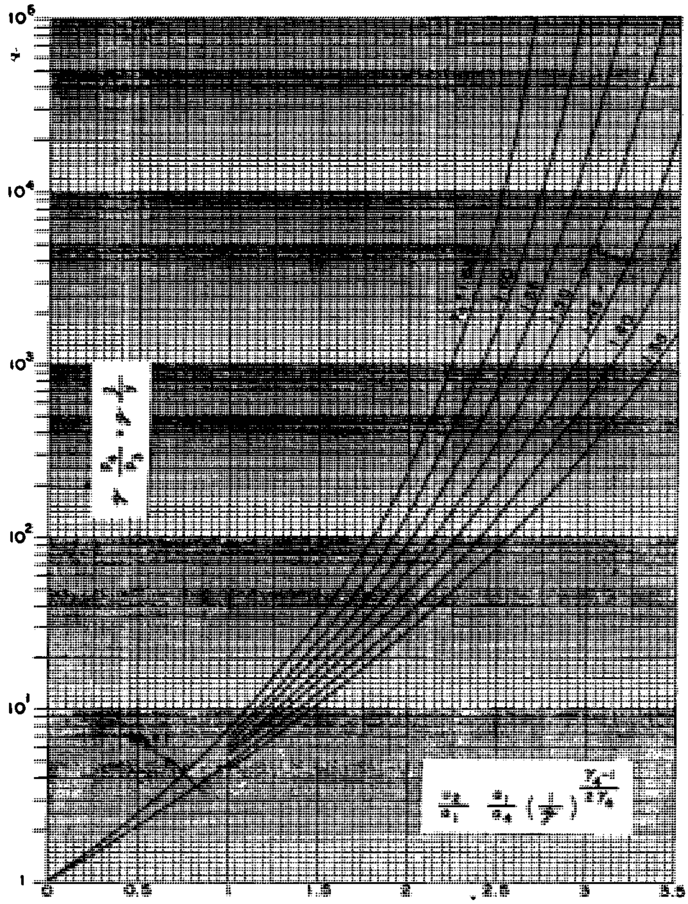

Figure 5. Curves for computing shock-tube performance. The point at which the cold flow becomes sonic is indicated.

Table 1 points out quite strikingly that the Mach number gain resulting from the use of a convergent transition section is not particularly large. The advantage of increasing sound velocity in the driver should be noted.

Comparisons of performance in convergent and straight tubes have been made by Lukasiewicz (1952), Resler, Lin & Kantrowitz (1952), and Yoler (1954) (see Alpher & White 1957 for a more detailed discussion

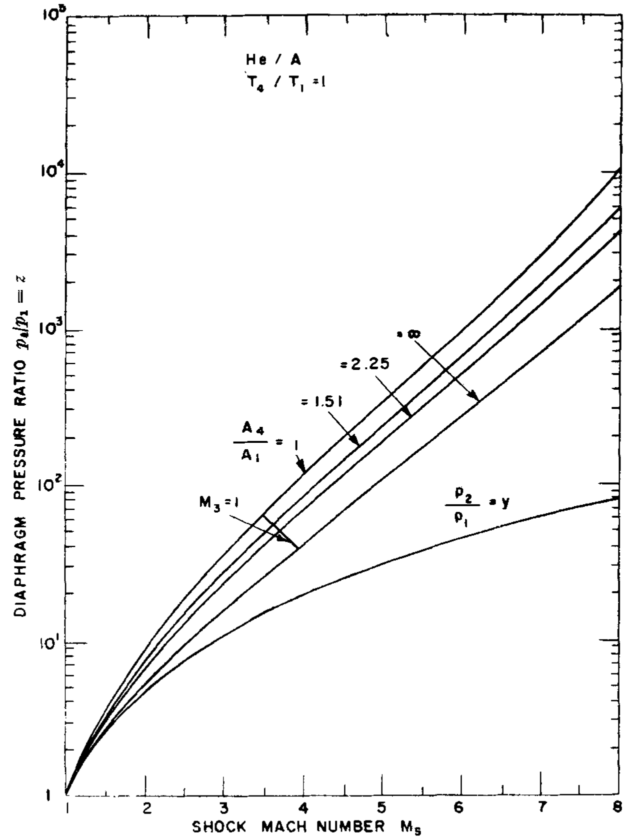

Figure 6. Diaphragm pressure ratio *vs* shock Mach number, for helium driving into argon at the same temperature. A plot of shock strength p_2/p_1 *vs* shock Mach number is included for reference.

	Driver-driven gas combination	$A_4/A_1 = 1$	1·51	2·25	∞
$T_4/T_1 = 1$	N_2/N_2	6·18	6·34	6·47	6·76
	N_2/A	7·48	7·69	7·84	8·20
	He/N_2	10·9	11·3	11·6	12·5
	He/A	12·8	13·3	13·7	14·7
	H_2/N_2	22·6	23·2	23·6	24·7
	H_2/A	27·5	28·3	28·8	30·1
$T_4/T_1 = 2$	He/N_2	14·8	15·4	15·9	17·1
	He/A	18·0	18·8	19·3	20·8
	H_2/N_2	31·9	32·8	33·4	34·9
	H_2/A	38·9	40·0	40·7	42·6

Table 1. Maximum values of shock Mach number M_s for $z = p_4/p_1 \to \infty$.

of their work). Lukasiewicz obtains limiting values of the equivalence factor g for $A_4/A_1 \to \infty$, but erroneously restricts them as holding only for equal cold flow Mach numbers M_3 in straight and convergent tubes. His work also suggests as a measure of gain the ratio of values of z in straight and convergent tubes required to achieve a given value of M_3. This does not appear to be a particularly useful measure since shocks of different strength will result. Resler, Lin & Kantrowitz discuss relative performance of the two situations from two viewpoints. First, one may regard the equivalence factor g as the 'gain in effective pressure' on driving a shock by using a steady flow (convergent) rather than an unsteady flow (uniform) transition section at the diaphragm. Second, they point out that a tube with a convergent section is 'equivalent' to a straight tube having an initial pressure ratio gz_c and an initial sound speed ratio $(a_4/a_1)g^{(\gamma_4-1)/2\gamma_4}$ (see equation (10)). Their discussion of these matters is quite brief and limited to the case of supersonic cold flow. Finally Yoler has used the equivalence factor g as though it were the gain factor G_M, which invalidates some of the data reduction and conclusions in his work.

Experimental work

Described below are some experiments with a shock tube in which the area ratio A_4/A_1 across the diaphragm section was alternatively 1·0 or 1·51. They show that the shock enhancement due to a convergent diaphragm section is satisfactorily predicted by the preceding analysis. Measured quantities were the initial pressures p_4 and p_1, and the shock velocity as a function of distance from the diaphragm. The shock tube had a driven section $3\frac{1}{4}$ in. square in cross-section and 40 ft. long. The driver was circular in cross-section, with a 4·5 in. inside diameter, and is 6·5 ft. long. Driver gases were helium and hydrogen, while driven gases were air, nitrogen, and argon. The most extensive data were obtained with helium/air, and only these will be reported here since the experiments with other gas combinations merely corroborated these results. In all tests the driver pressure was slowly raised until the diaphragm ruptured. The diaphragms were clamped at the driver end of the transition section, and were generally of 0·010 to 0·030 in. thickness stainless steel scored in a cross, one-third to a half of the thickness being removed by the scoring tool. Driver pressures were in the range of 100 to 800 lb./in.^{2} and were measured with a calibrated Bourdon gauge. Driven section pressures were measured with a manometer for $p_1 > 50$ mm of mercury, a Wallace and Tiernan absolute pressure indicator for 50 mm $> p_1 >$ 2 mm, or a McLeod gauge for $p_1 < 2$ mm.

Since the processes of shock formation and attenuation cause the shock velocity to change with distance from the diaphragm, instrumentation was devised to enable measurement of the shock velocity as a function of position in the tube, and hence to determine the maximum shock strength wherever it occurred relative to the diaphragm. The arrival of the shock at an instrument station along the tube was detected by a thin-film heat detector of the sputtered platinum type (Rabinowicz, Jessey & Bartsch 1956). To permit a number of such signals from different stations to be coupled to a recording system, it was desirable to lock out signals subsequent to the first from each station, and also to make the duration of this first signal very short. The heat detector output was amplified and fed to a 6D4 thyratron (the more commonly used 2D21 thyratron was found to be unsuitable due to its having firing delays of from 8 to 20 microseconds for weaker signals). The outputs from six of these thyratrons were fed through individual decoupling diodes to a blocking-oscillator type of pulse generator. Hence, through two such circuits, brief pulses were generated corresponding to shock arrivals at up to twelve stations spaced along the tube at 32·6 in. intervals. A vertical raster pattern was formed on the screen of a cathode-ray oscilloscope by connecting to the y-input a crystal-controlled sawtooth voltage generator of 100 microseconds period, the x-deflection being actuated by the oscilloscope's time base with a much longer period of about 10 milliseconds. In this manner about 500 cm of sweep at a writing speed of 20 microseconds/cm were obtained for a single sweep of the oscilloscope's time base. Time markers at 10 microsecond intervals were applied through intensity modulation of the oscilloscope. The amplified and shaped (i.e. shortened and freed from extraneous signals following the initial one) pulses originating from the heat gauges were applied directly to the x-plates of the oscilloscope, and so caused horizontal breaks in the vertical raster. The oscilloscope was triggered by the output from a barium–titanate transducer, which was fixed in the wall of the shock tube near the diaphragm and was sensitive to mechanical vibrations of the tube as the diaphragm broke. The shock velocity at different positions in the tube could readily be deduced from a photographic record of the raster, on which time intervals could be measured with a possible error of about a microsecond.

The shock tube as constructed had an area ratio $A_4/A_1 = 1{\cdot}51$. For these experiments an area ratio of unity was obtained by inserting down the centre of the driver a wooden dowel which terminated short of the diaphragm. This resulted in quite dissimilar cross-sections in the driver and driven parts of the tube, but permitted use of the same diaphragms as before the modification, so that the mechanics of the rupturing diaphragm was not a variable in the comparison.

In general a rapid acceleration of the shock to a maximum velocity was noted relatively near the diaphragm, followed by a gradual deceleration as the shock proceeded down the tube. Since the treatment in the present paper takes no account of shock formation and attenuation processes, the maximum shock velocity observed was judged to be that most suitable for comparison with the theoretical results. Since this observed value is actually the average over a significant interval, it is in general slightly smaller than the actual peak velocity.

The data are shown in figure 7. Note that the experimental shocks in each case are somewhat weaker than the theoretical predictions, but that the shock enhancement due to a convergent transition section is in excellent agreement with theory.

Our experiments have been continued to the study of stronger shocks than those described here; and with the present shock tube the indications are that, for diaphragm pressure ratios above about 1000 with hydrogen

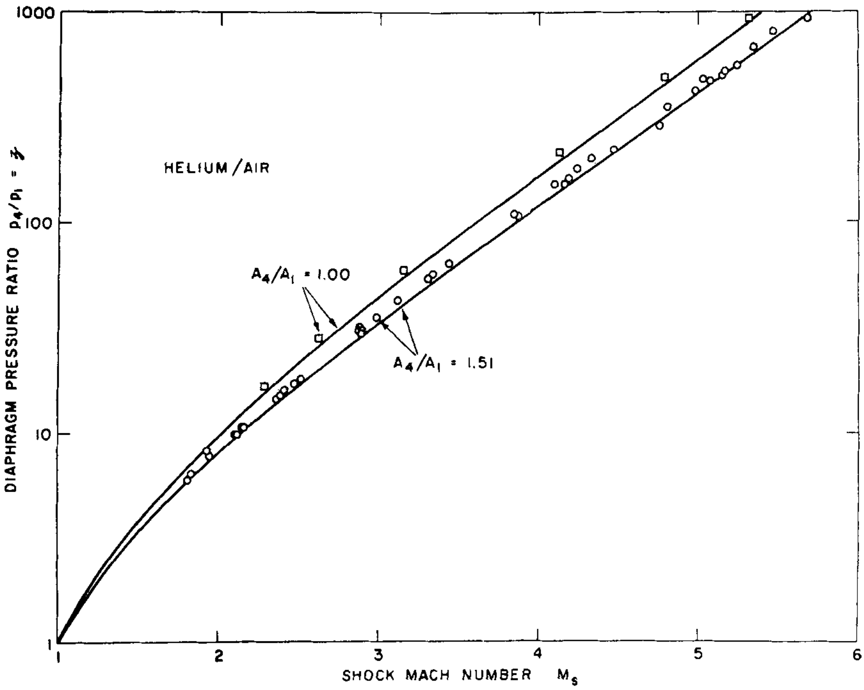

Figure 7. Comparison of ideal shock-tube theory with experiment for a 3¼ in. square shock tube to demonstrate the effect of a convergence at the diaphragm section.

or helium as the driver gas, the performance of the tube can no longer be depicted by an ideal theory. Shocks stronger than predicted by ideal theory are observed, and the maximum shock velocity in an experiment can occur quite far from the diaphragm. To explain such observations, one must consider the finite time for diaphragm rupture, mixing effects in the contact zone, shocked gas non-ideality, and wall attenuation effects. Nevertheless, even with these stronger shocks, the enhancement due to convergence appears to be predicted fairly accurately by ideal theory.

References

ALPHER, R. A. 1957 The Saha equation and the adiabatic exponent in shock wave calculations, *J. Fluid Mech.* **2**, 123.

ALPHER, R. A. & WHITE, D. R. 1957 Ideal theory of shock tubes with area change near diaphragm, *General Electric Research Laboratory, Schenectady, New York, Report* no. 57–RL–1664.

BANNISTER, F. K. & MUCKLOW, G. F. 1948 Wave action following sudden release of compressed gas from a cylinder, *Proc. Instn Mech. Engrs.* **159**, 269, DÖRING, W. 1949 Die Geschwindigkeit und Struktur von intensiven Stosswellen in Gasen, *Ann. d. Phys.* **6**, 133.

HOOKER, W. J. & WHITE, D. R. 1955 Design considerations for shock tubes generating hypersonic flow ($M > 6$), *General Electric Research Laboratory, Schenectady, New York, Chemistry Research Department Mem. Rep.* no. C–55–120.

LIEPMANN, H. W. & PUCKETT, A. E. 1947 *Introduction to Aerodynamics of a Compressible Fluid.* New York : Wiley.

LIGHTHILL, M. J. 1957 Dynamics of a dissociating gas, Part I, equilibrium flow, *J. Fluid Mech.* **2**, 1.

LUKASIEWICZ, L. 1952 Shock tube theory and application, *National Aeronautical Establishment, Ottawa, Report* no. 15.

RABINOWICZ, J., JESSEY, M. E. & BARTSCH, C. A. 1956 Resistance thermometer for transient high-temperature studies, *J. Appl. Phys.* **27**, 97.

RESLER, E. L., LIN, S. C. & KANTROWITZ, A. 1952 The production of high temperature gases in shock tubes, *J. Appl. Phys.* **23**, 1390.

WALLACE, F. J. & MITCHELL, R. W. S. 1953 Wave action following the sudden release of air through an engine port system, *Proc. Instn Mech. Engrs.* (B) **1B**, 8 & 343.

WALLACE, F. J. and NASSIF, M. H. 1954 Air flow in naturally aspirated two stroke engines, *Proc. Instn Mech. Engrs.* **168**, 515.

YOLER, Y. A. 1954 Hypersonic shock tube, *California Institute of Technology, Guggenheim Aeronautical Laboratory, Hypersonic Wind Tunnel Project, Mem.* no. 18.